SENSITIVITY ANALYSIS, DESIGN, INSTRUMENTATION, AND EXPERIMENTAL VALIDATION OF A NOVEL LABYRINTH SEAL RIG

T. Kluge - L. Wein* - R. Schmierer† - J.R. Seume**

* Institute of Turbomachinery and Fluid Dynamics, Leibniz University Hannover, Hanover, Germany, kluge@tfd.uni-hannover.de
† MTU Aero Engines AG, Munich, Germany

ABSTRACT

Measurements of the discharge coefficient of labyrinth seals reveal a strong sensitivity of the cavity flow to even small changes in geometrical parameters. It is shown that accurate measurements of the seal clearance are required to model the flow with a degree of certainty, which permits further conclusions. Based on accurate representations of the geometry in CFD models, it can be demonstrated that RANS flow solvers have substantial deficits in correctly predicting labyrinth seal flow. A novel test rig has been designed and put into operation for studying the labyrinth seal leakage flow in detail using temperature and pressure as well as optical flow velocity measurement methods. The rig uses a rotating disc with a labyrinth seal on its outer perimeter, and an annular flow channel to represent the shroud cavity. Homogeneity of the inlet and outlet boundary conditions is verified by means of circumferentially and radially distributed measurements of the total temperature and pressure. The rig mirrors the geometrical and aerodynamic parameters of the cavities in an axial turbine, which will subsequently be used for further investigations.

KEYWORDS

Labyrinth seal, cavity flow, discharge coefficient, turbomachinery, turbulence models

NOMENCLATURE

A	area	R	radius	ε	relative error
C_D	discharge coefficient	R_i	specific gas constant	κ	isentropic exponent
c	radial clearance	r	grid refinement ratio	μ	dynamic viscosity
K	swirl ratio	T	temperature	Π	pressure ratio
$\dot{m}$	mass flow	Re	Reynolds number	norm	normalised
p	pressure	U	rotational speed	tot	total
p	mathematical order	v_Θ	mid-section circumf. velocity	stat	static

INTRODUCTION

Modern turbomachinery is already highly efficient. According to Cumpsty (2010), no major improvement is expected unless unsteady aerodynamics are considered during the design phase. In light of this, the interaction of cavity flows with the main flow in turbomachinery becomes increasingly important. As shown by Biester *et al.* (2012), the interaction of the cavity flow with the main flow at re-entry after flowing through the labyrinth seal of a shrouded rotor introduces mixing losses, and increases the incidence of the stator downstream. In Biester *et al.* (2012),

0.9 % of the total mass flow rate passes through the labyrinth seal, not performing work on the rotor and reducing the isentropic efficiency of the stage by 2.5 %. Both the main flow and the cavity flow are expected to be highly unsteady and turbulent. Due to the large size of conventional pneumatic and temperature probes compared to engine-relevant cavity geometries, measurements obtained within the cavity or the mixing zone with the main flow cannot be assumed accurate due to unsteadiness and blockage. Consequently, extensive time-resolved numerical simulations are required to understand the mixing process and to identify possible design improvements. However, the accuracy of many current computational models is not sufficient to understand the influence modifications in the cavity design.

Computational modelling of the leakage flow interaction

Giboni *et al.* (2004) investigated the interaction of the cavity flow and the main stream in a $1^1/_2$-stage axial turbine by means of experiments and time-resolved numerical simulations. Their validation of the numerical model with hot wire measurements behind the rotor shows that CFD can capture trends correctly, e.g. the pitch-angle distribution, but fails to predict the correct amplitude of variation in time. Furthermore, the radial penetration of the leakage jet into the passage is under-predicted, i.e. too close to the shroud. Similar results are obtained by Henke *et al.* (2016) in a $1^1/_2$-stage low pressure turbine when comparing measurements using pneumatic five-hole probes to time-resolved numerical simulations. This may be caused by an inaccurate prediction of the flow in the labyrinth seal, the prediction of the flow close to the end-walls, or the prediction of the mixing of both flows. In order to identify the modelling deficits observed in Giboni *et al.* (2004) and Henke *et al.* (2016) the flow through the labyrinth seal and through the rotor need to be investigated separately. This paper is focussed on the prediction of the flow through the labyrinth seal.

Labyrinth seal test rigs

To validate the numerical models experimental data is required. With the exception of test rigs that do not account for the rotation of the blade shroud, most test rigs investigating labyrinth seals are restricted to global measurements of the discharge behaviour. Detailed measurements at discrete locations within the seal are not provided. For example, Iwatsubo *et al.* (1982) performed measurements of the leakage mass flow rate and static pressure in a straight-through labyrinth seal with two cavities. Gamal and Vance (2008) reported experimental results of the leakage mass flow rate and seal pressure ratio for various straight-through seal configurations. Both investigations yielded valuable insight into the leakage behaviour of labyrinth seals. However, the interaction with the main stream of a turbine can be significantly influenced by small changes in the width and the position of the leakage jet, which in turn might not influence the discharge behaviour of a labyrinth seal test rig. Thus, detailed measurements of the pressure and the velocity field inside the cavities are required.

One such investigation consists of the experiments conducted by Denecke *et al.* (2005). They, as well as others (e.g. Willenborg *et al.*, 2001; Schramm *et al.*, 2004), performed measurements in a stepped labyrinth seal test rig at engine-relevant Reynolds numbers. In Denecke *et al.* (2005) non-intrusive LDV measurements in the second of three cavities have been published. This test case has been used by Tyacke *et al.* (2012) and Wein *et al.* (2017) for the validation of computational results. Both investigations have shown that large discrepancies between computational and experimental results can occur without identifying the specific modelling deficit. Since only time averaged velocity components have been reported, the data for

the analysis of turbulence models is insufficient. Thus, even more detailed measurements of the flow in the cavities of the labyrinth seal are required. To this purpose, a new labyrinth seal test rig is introduced in this paper.

SENSITIVITY ANALYSIS

It is known, that the discharge behaviour of a labyrinth seal is influenced by small changes in the design of the seal clearance. However, the clearance can only be measured with limited accuracy. In order to quantify the sensitivity of certain results on measurement uncertainties of the geometry, CFD combined with finite element simulations are used.

Numerical Setup

Steady-state simulations have been conducted using TRACE, a flow solver for turbomachinery applications developed by the Institute of Propulsion Technology of the German Aerospace Center (DLR) in cooperation with MTU Aero Engines AG. The working fluid has been modelled as an ideal gas with a temperature dependent dynamic viscosity according to Sutherlands-Law. At the inlet circumferentially averaged radial profiles of the total pressure, total temperature, and flow direction have been specified. Based on measurements, a turbulence intensity of $2\,\%$ was defined. However, it can be shown that the inlet turbulence has a negligible influence on the flow inside the labyrinth seal, and that most turbulence is produced in the shear layer of the rotating disc, as well as in the expanding leakage jet downstream of the seal clearances. At the outlet, a circumferentially averaged static pressure with a radial equilibrium boundary condition was defined. The boundary layers are assumed to be fully turbulent, i.e. transitional effects are neglected and the walls are assumed to be adiabatic. As noted in previous studies, the assumption of adiabatic walls is negligible compared to the measurement uncertainties of the results discussed here. To minimise discretisation errors, a second order accurate Fromm scheme (Darwish, 1993) was selected for discretisation of spatial derivatives of the convective term. The Fromm scheme is bounded by the van Albada limiter (van Albada *et al.*, 1982). For the viscous fluxes, a second-order accurate central difference scheme was used.

Turbulence is accounted for with two-equation eddy viscosity models. The statistical two equation k-ω turbulence model described by Wilcox (1998) is used as a reference, due to its frequent use for the simulation of low-pressure turbines with cavities (Biester *et al.*, 2011; Mahle and Schmierer, 2011). The second turbulence model applied herein is the shear stress transport (SST) turbulence model as described in Menter (1994) to show the sensitivity on turbulence modelling and to motivate further analysis.

Domain and spatial discretisation

As shown in Fig. 1 the computational domain encloses the rig from the inlet to the outlet plane. A circumferential sector of 1° is used with periodic boundary conditions in circumferential direction. Hence, the rig is assumed to be rotationally symmetric, neglecting possible eccentricity due to manufacturing deviation or deformation during operation. An orthogonal H-Type blocking with an O-Grid along the walls is used to resolve the boundary layer, cf. Fig. 1. In the direction normal to the wall $y^+ \leq 1$ is adhered to, and the cell size increases with a factor of 1.2. Due to the high acceleration, turning, and detachment appropriate resolution and grid quality in the clearance is necessary. Therefore, the non-dimensional axial cell size in the clearance is $\frac{\Delta x}{c} \leq 0.06$. In the rest of the domain an axial cell size of $\frac{\Delta x}{c} \leq 0.6$ is selected and three cells are used in circumferential direction to obtain a quasi three-dimensional solution.

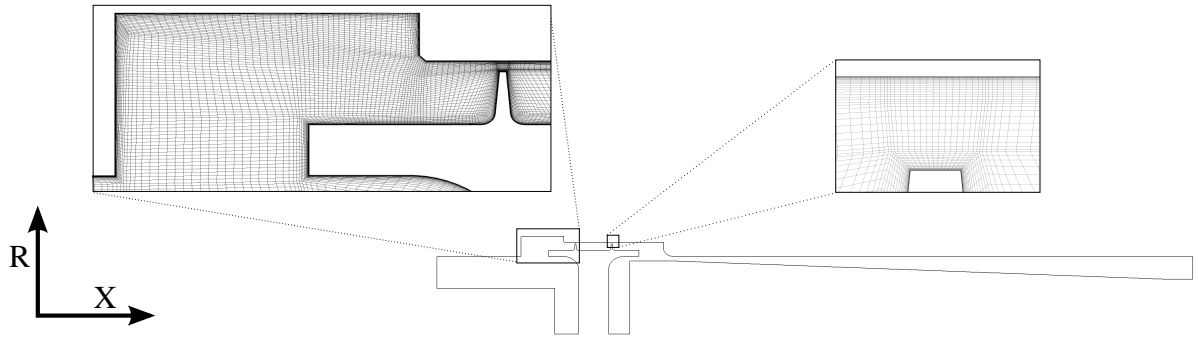

Figure 1: **Spatial discretisation of the computational grid**

Before the sensitivity on measurement uncertainties is evaluated, the sensitivity of the results on the spatial discretisation is evaluated by means of the grid convergence index (Roache, 1994) for the discharge coefficient. The discharge coefficient given by

$$C_{\mathrm{D}} = \frac{\dot{m}}{\dot{m}_{\mathrm{ideal}}} \tag{1}$$

relates the measured leakage mass flow rate $\dot{m}$ to an ideal leakage mass flow rate $\dot{m}_{\mathrm{ideal}}$. The latter is defined as the mass flow rate through an ideal nozzle

$$\dot{m}_{\mathrm{ideal}} = \frac{p_{\mathrm{tot,inlet}} \cdot A}{\sqrt{T_{\mathrm{tot,inlet}}}} \cdot \left(\frac{p_{\mathrm{stat,outlet}}}{p_{\mathrm{tot,inlet}}}\right)^{\frac{1}{\kappa}} \cdot \sqrt{\frac{2\kappa}{R_i\,(\kappa-1)}\left[1-\left(\frac{p_{\mathrm{stat,outlet}}}{p_{\mathrm{tot,inlet}}}\right)^{\frac{\kappa-1}{\kappa}}\right]}, \tag{2}$$

where A is the cross sectional area of the clearance. The reference grid with approximately 220,000 nodes predicts a discharge coefficient of $C_{\mathrm{D}} = 0.564$. The prediction of C_{D} is almost independent of the spatial discretisation, as shown in Tab. 1. Based on the data the coarsest grid appears to be sufficient for the investigation of the influence of variations of the clearance on the discharge coefficient and is used for all further studies in this paper.

Table 1: **Grid convergence index (GCI) and Estimated Extrapolated Relative Error (EERE) for the discharge coefficient after Roache (1994)**

$r_{12} = r_{23}$	ε_{12}	ε_{23}	p	GCI_1	GCI_2	GCI_3	EERE_1	EERE_2	EERE_3
0.5	0.004	0.003	2	$-5.9 \cdot 10^{-5}$	$-3.5 \cdot 10^{-5}$	$-2.1 \cdot 10^{-5}$	0.011	0.006	0.004

Sensitivity to geometric variations

The clearance can be predicted by analytical considerations and white-light-scans of the actual geometry with an uncertainty of 2 % of its value. Table 2 shows that the numerical prediction of the discharge coefficient is sensitive to this range of geometric variations, as may be expected. The discharge coefficient ranges as $C_{\mathrm{D}} = 0.564 \pm 0.01$ when the clearance of both throttlings is increased or decreased simultaneously. Furthermore, cylinder form tolerances may lead to a convergent or divergent configuration, i.e. with the clearance c of both throttling points

Table 2: **Sensitivity of the discharge coefficient on geometric measurement uncertainties**

Clearance configuration	Experiment	Reference $k-\omega$	Parallel 2%	Parallel -2%	Convergent $\pm 1.75\%$	Divergent $\pm 1.75\%$	Reference SST
$\mathbf{C_D}$	0.572 $\pm$0.01	0.564	0.576	0.553	0.564	0.564	0.655

differing by 1.75 % of the clearance height. The convergent clearance configuration refers to a situation in which the first clearance is larger. However, neither configuration leads to changes in the discharge coefficient C_D indicating that the influence of the clearance on the leakage mass flow rate is almost linear in this range of geometric variation. Nonetheless, it may be expected that the convergent or divergent clearance have an influence on local flow parameters, particularly the pressure drop across the first and second clearance, and the aeroacoustic and aeroelastic behaviour of the seal. Therefore, more detailed measurements in the cavity are required.

DESIGN & INSTRUMENTATION

To study the flow inside the labyrinth seal cavities in greater detail than previously possible and to validate computational models of the flow, a new labyrinth seal test rig has been designed and put into operation at the Institute of Turbomachinery and Fluid Dynamics (TFD) at Leibniz University Hannover. The rig is designed to mirror the geometry of the blade tip region of an axial turbine configuration with a shroud diameter of 450 mm similar to that described by Henke *et al.* (2016). The test rig is designed with multiple purposes in mind, specifically (1) the experimental validation of numerical simulations, (2) providing a test bench for cavity flow measurement techniques to be used in the axial turbine at TFD, and (3) calibration of the labyrinth seal as a mass flow measuring orifice.

The rig features an annular inlet channel between inner and outer casing with a height equivalent to approximately 25 % of the blade span of the aforementioned axial turbine configuration. The shroud diameter, cavity and labyrinth seal geometry, rotational speed, and pressure ratio across the seal are chosen to be equal to the respective parameters of the axial turbine. The rotor blade row is replaced by a disc, thus forcing the entire mass flow through the labyrinth seal. All casing components are fabricated from the same aluminium alloy. The rotating components are made from a steel alloy.

The air mass flow to the test rig is provided by a screw compressor, the excess mass flow being directed through a bypass duct. The operating points may be defined by the rotational speed or its reduced value, the mass flow or reduced mass flow, or the pressure ratio across the seal. The operating parameters of the test rig are summarised in Tab. 3.

A longitudinal section of the test rig is displayed in Fig. 2. The drawing is rotated in such way that the flow direction is from left to right, when in reality it is from bottom to top. The inlet and outlet measurement planes correspond to the inlet and outlet of the computational domain. Hence, inlet and outlet boundary conditions may be measured directly.

Upstream of the inlet plane, a volute casing is used to impose a circumferential velocity component on the flow similar to the first stator in Henke *et al.* (2016). At the design point, it has a swirl ratio of $K = {}^{v_\Theta}/_{U} = 0.08$, where U is the circumferential velocity of the rotor at the inner shroud diameter. Downstream of the outlet plane a second volute is used to collect the flow with minimal upstream disturbance. This design ensures a high level of circumferential

Working fluid	air
Couette Reynolds number after Denecke *et al.* (2005)	77065
Axial Reynolds number after Denecke *et al.* (2005)	17100
Taylor number after Waschka *et al.* (1990)	13660
Rotational speed	7000 rpm
Total pressure ratio	1.28
Inlet temperature	approx. 298 K
Max. inlet static pressure	0.5 bar

Table 3: **Operating parameters of the labyrinth seal test rig**

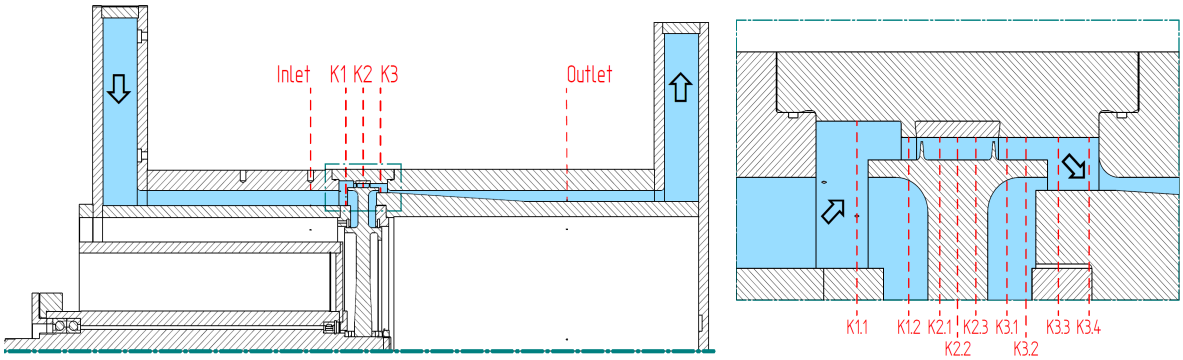

(a) (b)

Figure 2: **(a) Longitudinal section of the test rig (rotated 90°) with flow from left to right and (b) detail view of labyrinth seal with flow path shaded**

homogeneity in the flow field, which allows comparison of experimental and numerical data computed in a partial model.

Instrumentation

The test rig is extensively instrumented with sensors for steady and unsteady pressure, temperature, and velocity measurements. The mass flow is measured both upstream and downstream of the test rig. A thermal mass flow meter (expanded uncertainty of $\pm 2\,\%$ of the reading) downstream of the test rig represents the reference mass flow measurement, eliminating any leakage which may escape through the shaft bearings. A secondary mass flow measurement is recorded using a calibrated Venturi nozzle upstream of the test rig.

The inlet and outlet boundary conditions are determined experimentally by static pressure measurements at the inner and outer casing (i.e. the inner and outer confinement of the annular channel), total pressure measurements in five and three radial positions in the inlet and outlet plane, respectively, and by total temperature measurements in three radial positions. All of the above are measured in six circumferential positions.

The temperature and static pressure in the inlet and outlet cavity (K1 and K3, cf. Fig. 2) are measured by thermocouples and static pressure taps at the outer casing in six circumferential positions. Additional static pressure measurements are recorded in each measurement plane

depicted in Fig. 2(b), i.e. K1.1, K1.2, K2.1, K2.2, K2.3, K3.1, K3.2, K3.3, K3.4, where K2 is the vortex chamber of the labyrinth seal.

Time-resolved measurements of the unsteady static pressure are recorded with 200,000 samples per second at the outer casing wall. The measurements are located in two positions in the inlet cavity (K1.1), and four circumferentially staggered positions in the outlet cavity (K3.3) to allow cross-correlation of the pressure signals across varying angles. The turbulence intensity is measured by constant temperature anemometry in the axial positions K1.1 and K3.3, as well as on the inlet and outlet planes.

Optical access

The rig is designed to function as a test bed for particle image velocimetry (PIV) measurements, both within the exit cavity of the labyrinth seal and the mixing zone of the leakage jet and the main flow. In particular, the challenges of seeding the cavity flow for optical measurements and the optical access itself are subject to testing in this rig. To that end, windows are embedded in the outer casing for access to the inlet (K1) and outlet (K3) cavities as well as the inlet and outlet plane. This allows measurements of the two-dimensional, three-component velocity field in the meridional planes in all of the above positions via stereoscopic PIV. Results of these measurements will be the subject of future publications.

Radial deformation

As stated above the flow through labyrinth seals is highly sensitive to geometrical variations. Compared to rotors in turbomachinery, the disc of this rig experiences small deformations which are in the range of the uncertainty of available measurement methods. However, the deformation can be modelled analytically and based on finite element computations. According to the models a maximum radial deformation of the disc of approximately 4.5 % of the clearance height is expected due to the rotation of the disc, cf. Fig. 3. The undeformed geometry is measured by white-light-scanning to attain a highly accurate base geometry. Thermal strain of the disc has a significant impact in comparison with the deformation caused by centrifugal acceleration with up to 3.4 % of the clearance height for a temperature rise of $\Delta T = 10\,\mathrm{K}$. However, the temperature change is expected to be considerably lower based on measurements of the flow temperature. It is to be expected, that a non-uniform temperature distribution in the disc will cause a corresponding non-uniform expansion resulting in thermal stress. However, the available data suggests that the error due to the assumptions made is small. More detailed information is available for the casing temperature. For a temperature change at the rated pressure ratio of $\Delta T \approx 5\,\mathrm{K}$ the radial deformation of the outer casing ring is as high as 2.7 % of the clearance height due to an aluminium alloy used for the casing as opposed to the steel alloy used for the disc. Both thermal deformations compensate each other in part. Based on the available temperature measurements, the seal clearance is corrected for each measurement.

EXPERIMENTAL VALIDATION

Numerical computations reveal a strong sensitivity of the cavity flow to variations in the clearance height of labyrinth seals as demonstrated above. Moreover, modelling deficits in CFD depending on the turbulence model have been identified in literature based on discrete measurements within the labyrinth seal. The results of experiments in the test rig described above are presented in this section. For all measurements, the operating point is set and time is permitted for thermal equilibrium to be reached.

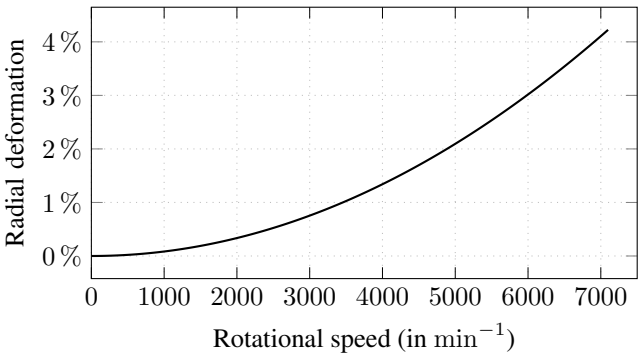

Figure 3: **Radial deformation of rotor disc (in per cent of initial clearance) based on finite element computation**

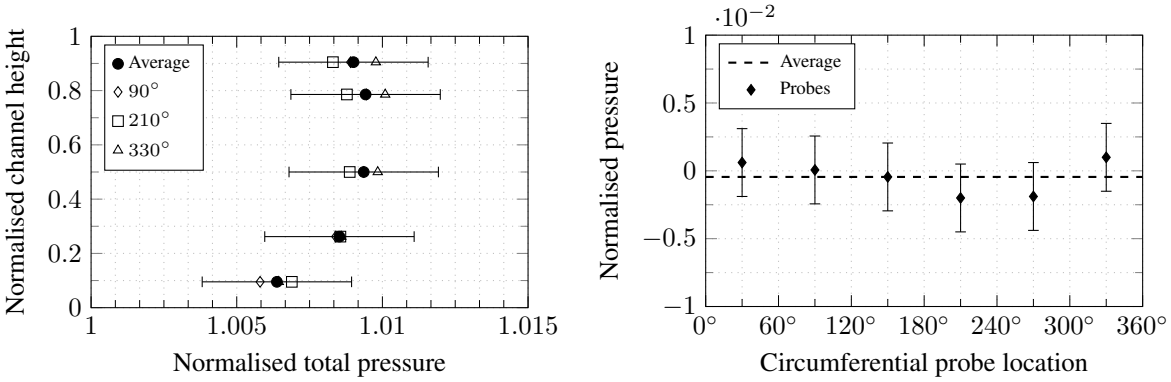

Figure 4: **(a) Total pressure in the Inlet plane for three circumferential positions across channel height and (b) static pressure in the Outlet plane, each with error bars indicating the expanded measurement uncertainty with a level of confidence of 95 % (JCGM, 2008)**

Homogeneity of inlet and outlet boundary conditions

The tongues of the volutes upstream of the inlet and downstream of the outlet can cause non-uniform inflow into or back pressure out of the measurement section. The inlet and outlet duct have been lengthened to avoid this influence. The circumferential change of the total pressure at the inlet is small compared to the measurement uncertainty, cf. Fig. 4(a). This indicates that the wake of the tongue is mixed out. Although the potential field of the tongue in the outlet-volute generates larger non-uniformities at the outlet, the non-uniformity is within the range of the measurement uncertainty. Therefore, the time-averaged flow in the rig is expected to be uniform in circumferential direction. Thus, circumferentially-averaged inlet and outlet boundary conditions for CFD post processing are valid. Consequently, a circumferential sector of 1° may be used for quasi three-dimensional steady-state RANS simulations with low computational cost.

Seal discharge characteristic

The discharge of the labyrinth seal was measured for varying rotational speeds and pressure ratios. The resulting discharge characteristic is presented in Fig. 5. The non-dimensional discharge of the seal, as expressed by the discharge coefficient C_D, is measured at various distinct rotational speeds of the disc and for various total-to-static pressure ratios across the seal. The change in clearance height due to centripetal acceleration was predicted analytically (and verified by finite element simulations). The thermal deformation of the outer casing was corrected, based on temperature measurements on the casing ring. No temperature measurements are available in the rotating system. However, a correction of the thermal deformation of the disc is performed based on the premise that the disc assumes the temperature of the flow. Any of these corrections merely change the level of the discharge coefficient proportionally to $1/A$.

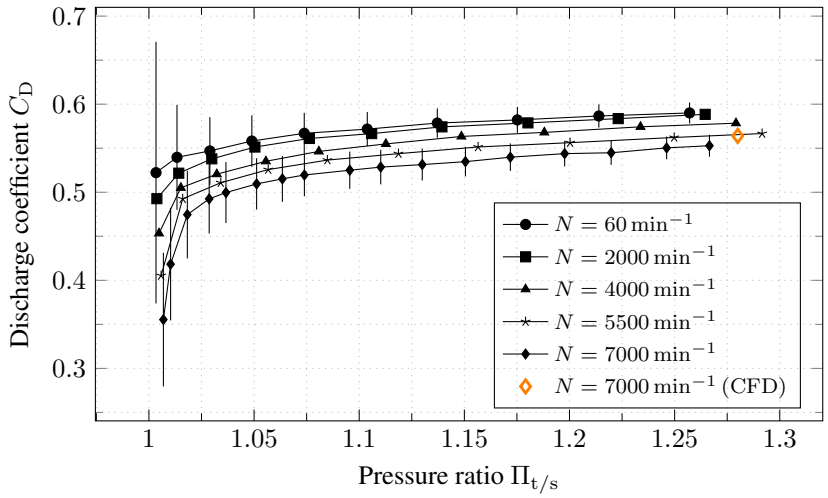

Figure 5: **Discharge characteristic of the labyrinth seal for varying total-to-static pressure ratios and rotational speeds including error bars indicating the expanded measurement uncertainty with a level of confidence of 95 %, cf. JCGM (2008) (for the minimum and maximum rotational speed only for greater clarity)**

The data indicates, that even the small radial deformation of the disc and resulting change in seal clearance (cf. Fig. 3) causes the discharge coefficient, i.e. the leakage mass flow, to vary strongly. At the rated pressure ratio of $\Pi = 1.28$ the change in radial clearance leads to a reduction of the discharge coefficient of approximately 6.5 % of the discharge at maximum clearance. This sensitivity on the clearance makes high demands on the measurement accuracy of the seal clearance. This necessity is still more pronounced in turbine experiments where the radial deformation is expected to be significantly larger.

The discharge coefficient predicted by CFD is validated by experimental data, cf. Fig. 5. The CFD model is corrected for the radial deformation to accurately represent the experiment. Due to a limitation of the inlet static pressure in the rig, the maximum pressure ratio at $7000\,\mathrm{min}^{-1}$ differs slightly from the CFD result. Nonetheless, when extrapolated the experimental characteristic matches the CFD result within the range of the measurement uncertainty.

Experimentally the effects of changes in clearance, local increase of temperature due to dissipation in shear layers, and the circumferential drag effect of the rotating surface on the fluid cannot easily be separated. This underlines the necessity for accurate measurements of the

radial clearance. The sensitivity on changes in the clearance height is analysed further in the next section based on numerical results.

Static pressure distribution

The static pressure distribution across the labyrinth seal serves as an indication of the loading on each individual sealing fin. To compare the results of experiment and CFD the static pressure on the shroud at the operating conditions given in Tab. 3 is normalised by

$$p_{\text{norm}} = \frac{p - p_{\text{inlet}}}{p_{\text{outlet}} - p_{\text{inlet}}} \tag{3}$$

and plotted in Fig. 6. The pressure distribution is also plotted for the geometric variation discussed above and different turbulence models.

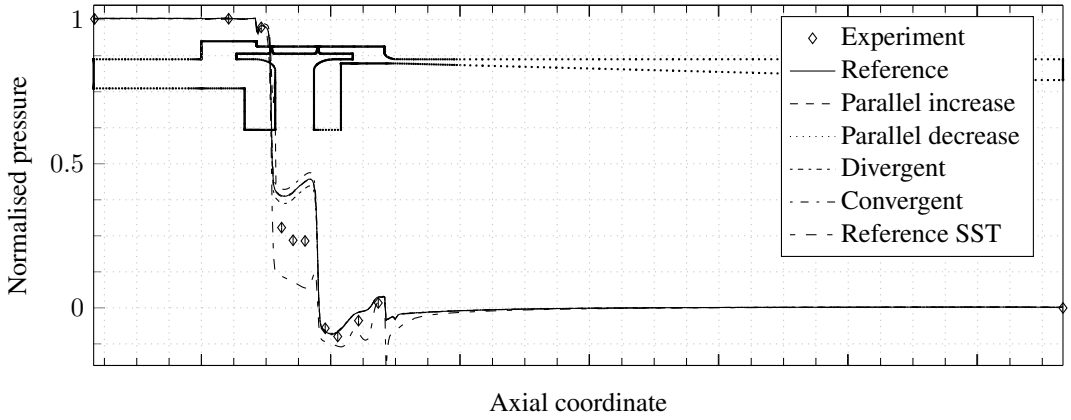

Figure 6: **Sensitivity of static pressure depending on geometric uncertainties and turbulence modelling (with error bars of experimental values approximately the size of the symbols)**

The measurements indicate that the loading of the first fin, i.e. the pressure drop across the first clearance, is approximately twice as high as the loading of the second fin. This is due to the low deflection of the leakage jet in the vortex chamber of the straight-through labyrinth seal and the high carry-over effect compared to stepped or interlocked labyrinth seals.

Despite the good prediction of the discharge coefficient, the reference CFD model over-predicts the static pressure in the vortex chamber by a minimum of 3,500 Pa. Furthermore, the CFD model predicts a pressure recovery in the vortex chamber while the leakage jet in the experiments continuously expands throughout the seal. This is likely related to a different widening of the leakage jet in the vortex chamber. Figure 6 also shows the sensitivity of the CFD results on the geometric variations discussed above. While the convergent and divergent clearance configuration have no measurable influence on the discharge coefficient, the loading of the fins changes by about $\pm$1,000 Pa. In contrast, a simultaneous increase or decrease influences the discharge coefficient, but does not influence the loading of the fins.

Discrepancies between CFD and experimental findings, however, are larger than the sensitivity to geometric variations stated above. This indicates a modelling deficit in the k-ω turbulence model, which is why the SST turbulence model has been tested accordingly. However, the discharge coefficient is over-predicted by approximately 13 % with the latter model as is

the loading of the first fin. Hence, the geometric measurement uncertainties attained are small in comparison to aerodynamic measurement uncertainties and the modelling deficits of RANS. Nevertheless, it is advisable to consider the geometric variations as uncertainties of the numerical results. Further investigation of impact of different turbulence models appears worthwhile when other uncertainties are minimised.

CONCLUSIONS

The flow through labyrinth seals has been shown to be highly sensitive to geometric variations due to changes in rotational speed. The discharge coefficient has been shown to vary significantly when the seal clearance is changed by 2 %. However, certain geometric variations do not result in changes in the discharge characteristic but are shown to influence the loading distribution of the seal.

A new test rig for detailed pressure, temperature and optical flow measurements in rotating labyrinth seals has been put into operation. The design goal of achieving circumferentially homogeneous flow conditions is met within the limits of measurement uncertainty. Though smaller than in a turbine rig, the radial deformations occurring in the test rig have a significant impact on the discharge characteristic.

The integral behaviour of labyrinth seals is modelled accurately when variations of the geometry are considered in the RANS-based numerical CFD model. However, not correcting for changes in seal clearances due to centripetal acceleration and thermal strain likely leads to incorrect numerical predictions of the flow field due to the high sensitivity of the seal leakage flow to geometric variations. It is therefore advisable to correct CFD models for known changes in the geometry. Uncertainties in the geometric parameters due to limited measurement accuracy may be treated as uncertainties of the numerical results.

In contrast, local flow parameters such as the pressure drop across the labyrinth seal are not predicted accurately. The experimental data show a different distribution of sealing fin loading. Additionally, the measurements indicate a difference in the expansion of the leakage jet downstream of the first fin when compared to computational models.

The modelling deficits observed for local flow parameters are large in comparison with the remaining uncertainty due to limitations in the representations of the true geometry present in the experiments. This confirms the observations reported in literature regarding the spread of the results of different turbulence models. These modelling deficits could lead to erroneous design decisions. Based on precise knowledge of the experimental conditions, further investigation of the flow in labyrinth seals is required including the use of higher order numerical methods such as large eddy simulation (LES). LES will be applied to the modelling of the present rig. Experimentally, a turbine test rig will be investigated next in order to achieve more realistic flow conditions through the seal.

ACKNOWLEDGEMENTS

The authors gratefully acknowledge the contribution of the DLR Institute of Propulsion Technology and MTU Aero Engines AG providing the TRACE code. Furthermore, the authors thank the Leibniz University Hannover (LUIS) and the North-German Supercomputing Alliance (HLRN) for their provision of computational resources. The investigations were conducted as part of the joint research programme AG Turbo and supported by the German Federal Ministry for Economic Affairs and Energy and MTU Aero Engines AG.

REFERENCES

Biester, M.H.O.; Henke, M.; Guendogdu, Y.; Engel, K.; and Seume, J.R. (2012): Unsteady Blade-Wake Interaction: A Correlation Between Surface Pressure Fluctuations and Loss Generation. In: Turbomachinery, Parts A, B, and C, vol. 8 of *Turbo Expo: Turbine Technical Conference and Exposition*, ASME, pp. 2743–2752.

Biester, M.O.; Mueller, L.; Guendogdu, Y.; and Seume, J.R. (2011): Time-Resolved Numerical Investigation of the Interaction of Labyrinth Seal Leakage and Main-Flow in a 1.5-Stage LP Turbine. In: Turbomachinery, Parts A, B, and C, vol. 7 of *Turbo Expo: Power for Land, Sea, and Air*, ASME, pp. 1623–1632.

Cumpsty, N.A. (2010): *Preparing for the Future: Reducing Gas Turbine Environmental Impact—IGTI Scholar Lecture*. In: J Turbomach, vol. 132(4):p. 041 017.

Darwish, M.S. (1993): *A New High-Resolution Scheme Based on the Normalized Variable Formulation*. In: Numer Heat Tr B-Fund, vol. 24(3):pp. 353–371.

Denecke, J.; Dullenkopf, K.; Wittig, S.; and Bauer, H.J. (2005): Experimental Investigation of the Total Temperature Increase and Swirl Development in Rotating Labyrinth Seals. In: Turbo Expo 2005, Parts A and B, vol. 3 of *Turbo Expo: Power for Land, Sea, and Air*, ASME, Reno, Nevada, USA, pp. 1161–1171.

Gamal, A.J.M. and Vance, J.M. (2008): *Labyrinth Seal Leakage Tests: Tooth Profile, Tooth Thickness and Eccentricity Effects*. In: J Eng Gas Turbines Power, vol. 130(1):p. 01 215.

Giboni, A.; Wolter, K.; Menter, J.R.; and Pfost, H. (2004): Experimental and Numerical Investigation Into the Unsteady Interaction of Labyrinth Seal Leakage Flow and Main Flow in a 1.5-Stage Axial Turbine. In: Turbomachinery, Parts A and B, vol. 5 of *Turbo Expo: Power for Land, Sea, and Air*, ASME, Vienna, Austria, pp. 983–992.

Henke, M.; Wein, L.; Kluge, T.; Guendogdu, Y.; Biester, M.; and Seume, J.R. (2016): Experimental and Numerical Verification of the Core-Flow in a New Low-Pressure Turbine. In: Turbomachinery, vol. 2B of *Turbo Expo: Turbomachinery Technical Conference and Exposition*, ASME, Seoul, South Korea, p. V02BT38A035.

Iwatsubo, T.; Motooka, N.; and Kawai, R. (1982): Flow Induced Force of Labyrinth Seal. In: NASA. Lewis Research Center Rotordyn. Instability Probl. in High-Performance Tubomachinery, NASA, pp. 205–222.

JCGM (2008): Evaluation of measurement data — Guide to the expression of uncertainty in measurement. JCGM 100:2008 (ISO/IEC Guide 98-3:2008).

Mahle, I. and Schmierer, R. (2011): Inverse Fin Arrangement in a Low Pressure Turbine to Impprove the Interaction Between Shroud Leakage Flow and Main Flow. In: Turbomachinery, Parts A, B, and C, vol. 7 of *Turbo Expo: Turbine Technical Conference and Exposition*, ASME, Vancouver, Canada, pp. 559–568.

Menter, F.R. (1994): *Two-Equation Eddy-Viscosity Turbulence Models for Engineering Applications*. In: AIAA Journal, vol. 32(8):pp. 1598–1605.

Roache, P. (1994): *Perspective A Method for Uniform Reporting of Grid Refinement Studies*. In: J Fluids Eng, vol. 116(3):pp. 405–413.

Schramm, V.; Denecke, J.; Kim, S.; and Wittig, S. (2004): *Shape Optimization of a Labyrinth Seal Applying the Simulated Annealing Method*. In: Int J Rotating Mach, vol. 10(5):pp. 365–371.

Tyacke, J.; Jefferson-Loveday, R.; and Tucker, P. (2012): On LES Methods Apllied to Seal Geometries. In: Turbomachinery, Parts A, B, and C, vol. 8 of *Turbo Expo: Turbine Technical Conference and Exposition*, ASME, Copenhagen, Denmark, pp. 2053–2065.

van Albada, G.D.; van Leer, B.; and Roberts, Jr., W.W. (1982): *A Comparative Study of Computational Methods in Cosmic Gas Dynamics*. In: Astron Astrophys, vol. 108(1):pp. 76–84.

Waschka, W.; Wittig, S.; and Kim, S. (1990): Influence of High Rotational Speeds on the Heat Transfer and Discharge Coefficients in Labyrinth Seals.

Wein, L.; Seume, J.R.; and Herbst, F. (2017): Improved Prediction of Labyrinth Seal Performance Through Scale Adaptive Simulation and Stream Aligned Grids. In: Turbomachinery, vol. 2B of *Turbo Expo: Turbine Technical Conference and Exposition*, ASME, Charlotte, USA, p. V02BT41A033.

Wilcox, D.C. (1998): Turbulence Modelling for CFD. 2nd edn., DCW Industries, La Canada, USA.

Willenborg, K.; Kim, S.; and Wittig, S. (2001): Effects of Reynolds Number and Pressure Ratio on Leakage Loss and Heat Transfer in a Stepped Labyrinth Seal. In: Heat Transfer; Electric Power; Industrial and Cogeneration, vol. 3 of *Turbo Expo: Power for Land, Sea, and Air*, New Orleans, USA, p. V003T01A010.